Incidence of Photovoltaics in Cities Based on Indicators of Occupancy and Urban Sustainability

3 authors:

Antonio Barragan
Universidad Politécnica Salesiana (UPS)
27 PUBLICATIONS   **49** CITATIONS

SEE PROFILE

Esteban Zalamea
University of Cuenca
27 PUBLICATIONS   **45** CITATIONS

SEE PROFILE

Julio Terrados
Universidad de Jaén
35 PUBLICATIONS   **483** CITATIONS

SEE PROFILE

Some of the authors of this publication are also working on these related projects:

Project El abastecimiento energético renovable desde recursos endógenos, en ciudades de paises en vías de desarrollo en el marco del metabolismo urbano. Caso de Estudio Cuenca, Ecuador. View project

Project Determinación de potencial de integración arquitectónica de captación solar activa en tipología constructiva de baja altura en centro patrimonial de ciudades andinas. Caso de Estudio Cuenca, Ecuador. View project

Incidence of Photovoltaics in Cities Based on Indicators of Occupancy and Urban Sustainability

Antonio Barragán-Escandón [1],*[ID], **Esteban Zalamea-León** [2][ID] **and Julio Terrados-Cepeda** [3][ID]

[1]   Department of Electrical Engineering, Universidad Politécnica Salesiana, Calle Vieja 12-30 y Elia Liut, Cuenca 010102, Ecuador

[2]   Facultad de Arquitectura y Urbanismo, Universidad de Cuenca, Cuenca 010103, Ecuador; esteban.zalamea@ucuenca.edu.ec

[3]   Department of Graphic Engineering, Design and Projects, Universidad de Jaén, 23071 Jaén, Spain; jcepeda@ujaen.es

*   Correspondence: ebarragan@ups.edu.ec; Tel.: +53-9990017601

check for updates

Abstract: Previous research has assessed the potential of solar energy against possible demand; however, the sustainability issues associated with the use of large-scale photovoltaic deployment in urban areas have not been jointly established. In this paper, the impact of photovoltaic energy in the total urban energy mix is estimated using a series of indicators that consider the economic, environmental and social dimensions. These indicators have been previously applied at the country level; the main contribution of this research is applying them at the urban level to the city of Cuenca, Ecuador. Cuenca is close to the equatorial line and at a high altitude, enabling this area to reach the maximum self-supply index because of the high irradiation levels and reduced demand. The solar potential was estimated using a simple methodology that applies several indexes that were proven reliable in a local context considering this particular sun path. The results demonstrate that the solar potential can meet the electric power demand of this city, and only the indicator related to employment is positive and substantially affected. The indicators related to the price of energy, emissions and fossil fuel dependency do not change significantly, unless a fuel-to-electricity transport system conversions take place.

Keywords: urban renewable energy; urban photovoltaics; urban solar potential

1. Introduction

Currently, cities are responsible for 75% of the total carbon dioxide emissions, which are the primary cause of global warming [1]. The energy demand of urban environments can be reduced or substantially met through the application of energy-efficient measures and renewable technologies [2,3]. Furthermore, since these measures can achieve energy independence and democratization for countries in terms of their import needs, the aggressive use of renewable energies (REs) can reduce emissions, create jobs and increase the gross domestic product [4]. Different possibilities for urban energy self-generation have been analyzed [5].

In recent years, the urban insertion of renewable energy production has resulted from the adoption of public policies, municipal incentives and the adoption of strategies at different scales and met relative success depending on local conditions [3,6]. Photovoltaics (PVs) present the greatest economic, social and environmental development opportunity and are considered the fastest growing technology [7]. Mainly large-scale solar farms have been developed, which occupy large plots of land and potentially impinge upon nature and food production [8,9].

Compared with distributed solar thermal (ST), PV electric power surpluses are more readily exported, which is primarily because heat storage from ST is complex, and considerable waste is produced when it is not used immediately. Wind technology for urban integration is not yet adaptable; urban development interferes with wind technology effectiveness through air current barriers. Moreover, wind technology, which includes moving parts and produces vibrations, is aesthetically questionable, acoustically contaminating, and visually distracting [10]. Geothermal energy requires a large ground area and is difficult to apply in populated spaces. Other urban technologies take advantage of waste and reduce the need for landfills; however, their conversion to useful energy may not be efficient and could cause environmental issues, such as greenhouse gas emissions [11].

Resources available in cities can be used to produce energy, however, the global impact of urban insertion has not been properly assessed. Therefore, employing sustainability indicators is important for evaluating the impact of the substantial insertion of PV systems into a city from an integrated energy perspective.

1.1. Photovoltaic Potential in Cities

Several methodologies have been developed to estimate the available and usable irradiation in urban areas [12]; moreover, multiple strategies have been developed to evaluate the ability of PVs to operate in a built environment [13,14]. Three-dimensional (3D) analyses have evolved to a state where they can be used to evaluate urban solar potential. Using 3D analysis methods, the effects of shadows and the surface layout of facades and roofs can be included [15,16], along with the urban density and surface orientation [17]. However, extensive human and computational resources are required to process geometrical information [16]. These methodologies require substantial resources for redrawing, including two-dimensional (2D) and 3D building surveys, aerial data processing and data discrimination, which are costly. The ground floor building occupancy of many municipalities is stored as vector data in databases and used as a tool for urban planning.

The energy that PVs can provide is closely related to the space available for their placement. Their orientation and potential shadowing are factors that can impact their effectiveness, and the location is relevant because buildings near the equatorial line receive irradiation on almost all roof surfaces. Additionally, at high latitudes, the irradiation on facades is more important.

The International Energy Agency (IEA) predicts that by 2050, PV installations integrated into buildings could supply 32% of urban consumption and 17% of the total power demand (IEA, 2014). In New York, PVs have the potential to generate economic benefits by avoiding distribution and transmission losses (Byrne, Taminiau, Kim, Seo, & Lee, 2015); moreover, they provide additional benefits related to the environment and health.

However, in the analyzed cases of large-scale urban PV deployment, the impact of PVs on total demand (not only electrical) was not determined. Table 1 lists the research assessing the urban PV potential. Although the methodologies and objectives in the studies varied, they showed that up to 100% of the demand can be supplied; however, achieving that potential energy supply depends on the consumption, endogenous resources and network conditions.

As noted, many studies worldwide have calculated the PV potential using techniques that are often applicable under local conditions (climate, urban topology, latitude, energy demand, the shape of the building) [27]. PV technology incorporated in urban areas contrasts with different building design aspects that prevent optimal solar availability. The PV potential is closely linked to the space available for the placement of PV panels. The orientation, slope and presence of shadows are other factors influencing the optimal capture of solar energy. Buildings near the equatorial line have the majority of the uptake on roofs; by contrast, in Mediterranean areas up to high latitudes, the facades are more propitious. Several characteristics of a city's physical location can be exploited to generate more suitable estimates for a specific location. Compared with recent studies, our proposal suggests that solar potential and the incidence of such energy systems should also be measured with sustainability indicators, which are generally applied at the regional or national level.

Table 1. The estimation of solar potential in cities.

City	Potential	Demand	Reference	Objective
Ostfildern (Germany)	45.00%	10.70 GWh	[18]	Analyses the performance of renewable energies (REs) in urban environments.
Ludwigsword (Germany)	18.00%	430.00 GWh		
Munich (Germany)	100.00%	20.00 kWh/m^2	[19]	Evaluates PV energy potential according to the building design.
Wageningen (Netherlands)	50.00% 66.00%	45.00 kWh/m^2 year	[20]	Investigates the self-supply potential with cities' own energy resources.
Kerkrade (Netherlands)	18.00%	481.00 GWh	[21]	Provides a methodology to identify energy sources that can be used within the city.
Karlsruhe (Germany)	9.05% **	410.00 GWh	[22]	Uses a method that calculates the PV economic potential of roofs and facades.
Zernez (Switzerland)	64.00%	7.40 GWh/year	[23]	Provides a framework for optimal photovoltaic energy integration in a villa.
Cities of Nepal	100.00%	1228.00 GWh	[24]	Evaluates the feasibility of electric power production with PV panels to supply unmet demand.
Ludwigsburg (Germany)	65.00%	3.54 GWh Panels located on roofs.	[25]	Calculates the potential of PVs to provide electricity based on a 3D model.
Dhaka (Bangladesh)	15.00%	773.41 GWh/year	[26]	Analyses the available roof area and models the energy system to determine the PV potential.

1.2. Sustainability Energy Indicators in Cities

The incorporation of PVs in a city is evaluated via indicators that allow us to compare the presence and status of public building policies aimed at promoting urban REs. The indicators are formulated according to the measurement requirements. The extrapolation of indicators used at the national and regional scales to urban areas is proposed because indicators that measure urban RE performance have not been defined [28–30].

The indicators applied in this study evaluate sustainability by modifying the energy matrix. The Organization for Economic Cooperation and Development (OECD) and the IEA [31] describe 30 indicators that can be used to analyze the energy situation in a country. Within this base, the Economic Commission for Latin America and the Caribbean (ECLAC), the Latin American Energy Organization (Organización Latinoamericana de Energía, OLADE) and the German Organization for Technical Cooperation (GTZ) [32] identified 8 sustainability indicators for Latin America.

Another study identified 29 indicators for the energy sector, including energy, social, economic and environmental factors [33].

The indicators applied to a given situation should be formulated based on the available information [31]. Indicators that use variables without synergy with other variables are preferred, i.e., indicators whose variables remain constant under variations in other variables.

In the literature, indicators capable of evaluating the variations in an urban energy model using REs were not detected. However, various reports have proposed indicators that measure the energy structure in countries that could be extrapolated. In Table 2, the indicators that measure proposed sustainability in cities are shown along with citations.

Table 2. The sustainability energy indicators.

Dimension	Indicator	Unit	Source
Economic	Autarchy	%	[32]
	Energy price	USD/BOE *	[33]
	Average energy price	USD/BOE	[33]
	Use of RE in energy supply	%	[32]
Environmental	Use of RE in electricity supply	%	[33]
	Energy purity	CO_2/BOE	[32]
Social	Employment	Jobs-year	[31]

* Barrel of Oil Equivalent.

1.3. Case Study

Cuenca city is located in the Andes mountain range near the equatorial line. The city is located between the geographical coordinates of $2°30'$ and $3°10'$ south latitude and $78°51'$ and $79°40'$ west longitude and at an average elevation of 2600 masl [34] (Figure 1). Approximately 2.28% (73 km^2) of its area (3190 km^2) is considered urban according to municipal legislation.
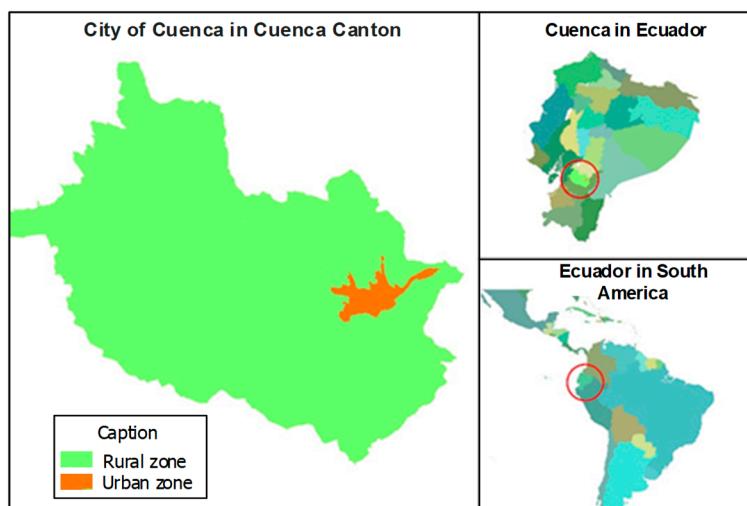
Figure 1. The geographic location of Cuenca Canton, urban area. Source: Based on information from INEC [35] and Jaramillo [36].

1.4. Irradiation Availability

The irradiation in Cuenca averages 4.19 kWh/m^2/day on a horizontal surface [37] (Figure 2). According to the scale proposed by Koo et al. [27], the city of Cuenca provides suitable solar resources for PV use. The maximum values occur in January, October, November and December. A reduction occurs between June and July since the region is located slightly south of the equator, and the reduction mostly arises from variations in cloudiness.
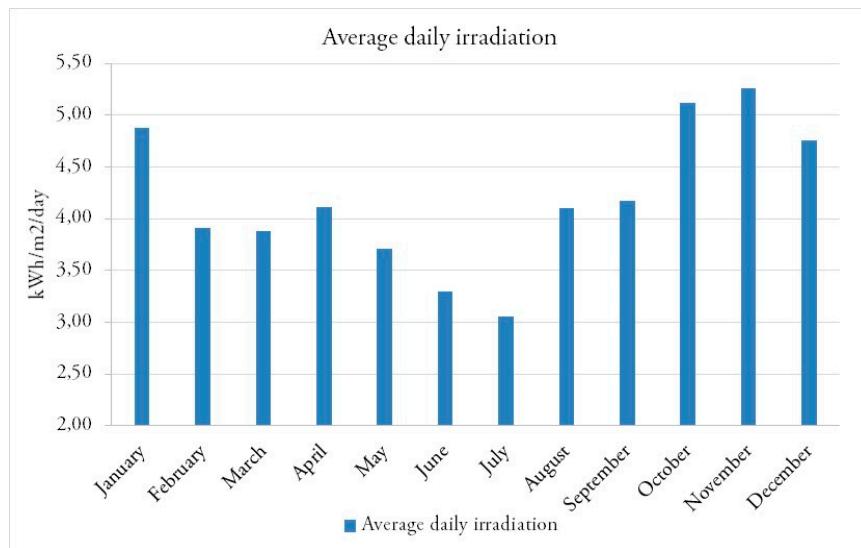
Figure 2. The average daily irradiation. Source: Based on NREL [37].

1.5. Electrical Demand

The South-Central Regional Electric Company provides urban services to the city [38]. The combination of electricity sources in Ecuador includes hydroelectric power (49%) and thermoelectric power (47%), with small amounts of wind, PV and biomass energy [39].

In 2015, the required electric service was 423.80 GWh (262.38 kBOE). The per capita consumption was approximately 3.89 GJ/inhabitant/year (1082.11 kWh/inhabitant/year) [38]. The residential sector was the largest consumer at 39%, followed by the industrial (23.59%) and commercial (22.72%) sectors.

The total energy demand from different sources is shown in Table 3. Consumption is strongly influenced by transportation, which accounts for 60%, followed by industry, housing and commerce at 20.76%, 13.72% and 3.15%, respectively. The primary sources are fossil fuel gasoline (GA) at 36.25%, diesel (DI) at 29.05%, liquefied petroleum gas (LPG) at 14.81%, oil fuel (OF) at 8.04% and natural gas (NG) at 2.19%, whereas electricity contributes approximately 9%. Although no precedents have been presented for an actual urban energy mix in Ecuador, the energy situation of the city of Cuenca is presented in Table 3 and proportionally is very close to the national consumption mix. [40].

Table 3. The energy balance of the city of Cuenca Canton (kBOE).

	EP *	NG	GA	DI	OF	GLP	Total
Production							
Import	282.13	59.47	984.85	789.35	218.49	402.46	2736.75
Export							
Total supply	282.13	59.47	984.85	789.35	218.49	402.46	2736.75
Distribution	−19.67	0.00	0.00	0.00	0.00	0.00	−19.67
Total transformation	−19.67						−19.67
Residential	102.34					270.39	372.73
Industry	61.89	59.47		127.33	216.55	98.68	563.92
Transportation			984.83	642.73			1627.56
Commercial	59.62	0	0	0	0	25.89	85.51
Street lighting	18.56	0	0	0	0	0	18.56
Other	19.98		0.02	19.29	1.93	7.49	48.72
Total demand	262.39	59.47	984.85	789.35	218.49	402.46	2717.00

* EP, electric power; NG, natural gas; GA; Gasoline; DI, diesel; OF, oil fuel, LPG, Liquefied petroleum gas.

In Figure 3, the information presented in Table 3 is shown in a Sankey diagram of the baseline situation in the city of Cuenca. Based on the model proposed by Barragán and Terrados [41], Figure 4 indicates the current urban model.
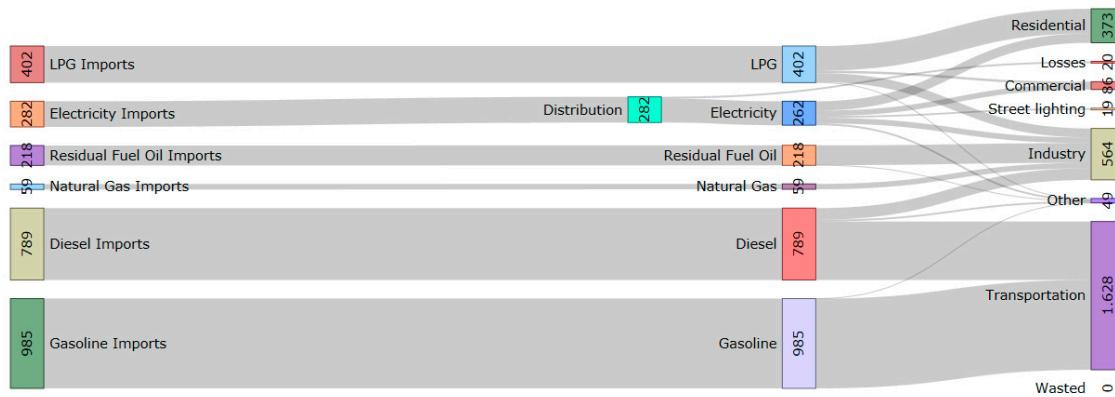

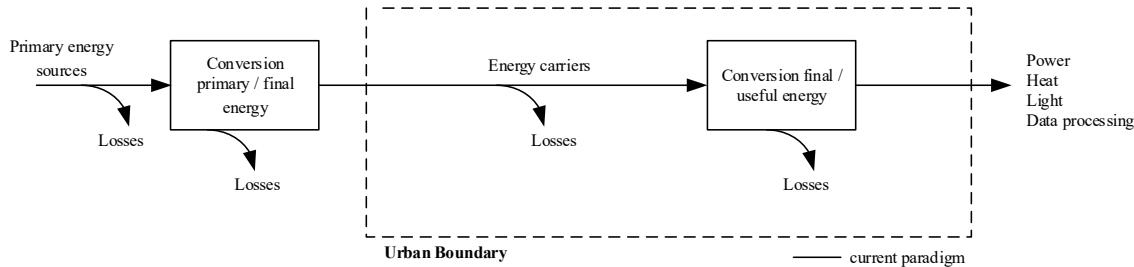**Figure 3.** The Sankey diagram of the energy situation in Cuenca.

Figure 4. The current energy model of Cuenca.

2. Methodology

To evaluate the urban solar potential in Cuenca, the potential roof exposure is analyzed at a latitude near the equator (2°54′ south). Under typical conditions, the irradiation exposure would be maximized by orienting the PVs towards the north at a very low slope. However, the results of a previous study showed that the ideal arrangement for production is towards the east because of the direct exposure to the sun and because cloudiness is statistically lower early in the morning [42]. By placing PVs at a typical roof inclination, the difference in annual production is only 7% below the optimal (east) to the least suitable (south) level, and the other orientations are between that [43]. This difference is marginal and implies that any direction of PV inclination is suitable for energy generation.

2.1. Technical Potential

The annual solar technical potential is established via Equation (1), as follows [28,44–46]:

$$P = A_{FV} \cdot I \cdot Fr \cdot \eta_r \tag{1}$$

where
　　P is the technical potential in kWh/year;
　　A_{FV} is the available area for placement on the roofs in m^2;
　　I is the average annual global irradiation in kWh/m^2;
　　F_r is the correction for architectural availability; and
　　η_r is the PV conversion for technological efficiency.

F_r is the reduction factor for restrictions in PV placement based on architectural availability or solar resources. The reduction factors (η_r) are included because not all irradiation is converted into

electricity, with conversion depending on the installation's PV efficiency and inverters as well as dirt and environmental conditions, which can affect the temperature of the cells and their corresponding efficiency [47,48]. Romero et al. [45] developed a set of reduction factors based on an extensive literature review, and they are used in this study as shown in Equation (2):

$$F_r = C_{con} \times C_{prot} \times C_{so} \times C_{or} \times C_{in} \times C_{SM} \times C_{FV} \times C_{ST}, \tag{2}$$

where

C_{con} represents the construction restrictions;

C_{prot} represents restrictions from historic buildings

C_{so} represents restrictions due to shadows;

C_{or} represents restrictions due to orientation;

C_{in} represents restrictions due to inclination;

C_{SM} represents the available spacing for the separation and maintenance paths of PVs in terraces;

C_{FV} represents the availability for PV placement; and

C_{ST} represents the availability for the placement of solar collectors.

Regarding the reduction factors for technical potential, Romero et al. [45] also included the factors that intervene in the conversion of irradiation to PV electricity. Equation (3) is used to calculate this reduction as follows:

$$\eta_r = \eta_{ef} \times \eta_{te} \times \eta_{or} \times \eta_{in}, \tag{3}$$

where

η_r represents the reduction factor of the solar potential;

η_{ef} represents PV efficiency;

η_{te} represents the losses from weather conditions (temperature and irradiation);

η_{or} represents losses from the angle of solar incidence; and

η_{in} represents losses in the network and installation during maintenance and from dirt.

2.2. Calculation of the Energy Sustainability Indicators

The indicators shown in Table 2 are obtained from the energy balance of the city and the socioeconomic data available for Ecuador.

2.2.1. Energy Autarchy

Autarchy measures the contribution of imports to the energy supply [32], and it is also defined as the degree of energy dependency since it correlates imports to the gross energy supply [29,49]. Equation (4) is used to calculate the weight of energy imports as follows:

$$AE = \frac{\sum_i^m IE_p + \sum_i^n IE_s}{O_E} \tag{4}$$

where

AE represents the autarchy (%);

IE_p represents the primary energy imports (BOE);

IE_s represents the secondary energy imports (BOE);

n represents the number of primary energy imports;

m represents the number of secondary energy imports; and

O_E represents the total gross energy supply (primary energy imports + secondary energy imports – primary energy exports – secondary energy exports + inventory variation – unused primary and secondary energy – secondary energy production) [44] (BOE).

2.2.2. Energy Price

The energy price (as expressed in Equation (5)) is obtained from the production costs plus profits (Ut) and taxes (Im) as follows:

$$PE_j = Ce * (1 + Ut) * (1 + Im),\tag{5}$$

where

PE_j is the price of energy resource j (USD/BOE);

C_e is the energy production cost (C_{pb} biofuel, C_{el} electricity or C_c heat) during its useful life (USD/BOE);

Ut is the business profit (%); and

Im corresponds to taxes imposed by the government (%).

The generation cost during the useful life is the average unitary cost in USD/kWh that should be paid for each unit produced to compensate for all the costs associated with the installation during its entire useful life and considering the monetary value each instant [50,51]. Using Equation (6), this cost is calculated as follows:

$$Ce = \frac{\sum_t [CI + O\&M_t] \cdot (1 + r)^{-t}}{\sum_t \left[Ene_t \cdot (1 + r)^{-t} \right]}\tag{6}$$

where

Ce is the energy production cost during the useful life of the system (USD/kWh);

Inv is the investment in the current year (including interest during construction and all supplementary elements and infrastructure) (USD/kWh);

$O\&M_t$ is the operation and maintenance cost in year t (USD/kWh);

r is the discount rate;

Ene_t is the energy produced in year t (kWh); and

t is the number of years of plant operation.

Using Equation (7), the influence of the plant size on costs is avoided since there are discrepancies caused by economies of scale as follows:

$$C_{T1}/C_{T2} = (S_1/S_2)^p,\tag{7}$$

where

C_{T1} and C_{T2} are the costs of the plants for sizes S_1 and S_2, respectively [52,53]; and

p is the growth factor, which depends on the type of process.

2.2.3. Average Energy Price to the Final Consumer

According to Garcia et al. [33], the average energy prices are calculated using Equation (8) as follows:

$$PME = \frac{\sum_{j=1}^m \sum_{k=1}^n PE_{jk} * E_{jk}}{\sum_{j=1}^m \sum_{k=1}^m E_{jk}}\tag{8}$$

where

PME is the average energy price (USD/BOE);

PE_{jk} is the price of energy resource k in sector j (USD/BOE);

E_{jk} is the amount of energy from resource k in sector j (BOE);

M is the number of consumer sectors; and

n is the number of energy resources required in the city.

2.2.4. The Proportion of Total Energy Consumption Provided by REs

The next indicator is the participation or contribution of REs to the urban energy matrix. Equation (9) is used to determine this indicator as follows [54]:

$$UR = \frac{\sum_i^m ER_i}{OE} \tag{9}$$

where

UR is the participation of REs in the total supply (%);
ER_i is the supply of renewable energy i (BOE);
O_E is the total gross supply of energy (BOE); and
m is the number of RE technologies.

2.2.5. REs in the Electric Supply

The indicator for the participation of REs in electrical production [30,33] is calculated by Equation (10) as follows:

$$URe = \frac{\sum_i^m ERe_i}{OEe} \tag{10}$$

where

URe is the participation of the RE in electric power generation (BOE);
ERe is the production of RE electricity with technology i (BOE);
OEe is the total electric production in (BOE); and
m is the number of RE technologies.

2.2.6. Purity Relative to the Use of Energy

The indicator relates CO_2 emissions to energy consumption [30,49]. Using Equation (11), the indicator *PRe* is obtained as follows:

$$PRe = \frac{CEC}{\sum_i^m DE_i} \tag{11}$$

where

PRe is the purity of the energy (ton CO_2/BOE);
CEC is the quantity of carbon dioxide emissions related to the energy demand (ton CO_2);
DE is the total energy demand (BOE); and
m is the energy resources required in the city.

The emissions related to demand (CEC) [55,56] are estimated via Equation (12) as follows:

$$CEC = \sum_i \sum_j \sum_n AL_{n,j,i} \times EI_{n,j,i} \times EF_{n,j,i} \tag{12}$$

where

$AL_{n,j,i}$ is the activity level related to fuel type n, equipment j and sector i;
$EI_{n,j,i}$ is the energy consumption related to fuel type n, equipment j and sector i; and
$EF_{n,j,i}$ is the emissions factor related to fuel type n, equipment j and sector i.

The emissions factors are those suggested by the Intergovernmental Panel on Climate Change (IPCC) [56].

2.2.7. Employment

The next indicator is used to compare the number of jobs related to the energy source, and it is estimated using Equation (13) as follows:

$$Em = \sum_{i}^{m} D_i * Ie_i \tag{13}$$

where

Em is jobs per year used by the energy industry;

Di is the energy resource demand i (BOE or GWh); and

Ie_i is the job factor of the energy resource i (jobs–year/BOE or jobs-year/GWh).

Wei et al. [57] established two indicators to calculate the number of jobs based on energy power for the following stages: (i) construction, installation and manufacturing (CIM) and (ii) operation and maintenance (OM).

Knowing the number of jobs created in a reference facility of a determined power (MW) for CIM and OM, these indicators are obtained for a plant if the useful life and plant factor are known using Equations (14) and (15) as follows:

$$CIM = \frac{CIM_I * N_I}{P_I} \tag{14}$$

where

CIM_I is the number of people required for the construction, installation and manufacturing of a reference plant [people-year];

N_I is the number of years used for the CIM of the reference facility (years);

P_I is the power capacity of the reference facility (MW); and

CIM is the personnel required for the construction of the reference infrastructure MW during N_I years (people-year/MW).

Using Equation (15), the number of OM jobs can be obtained for the construction of a reference installation MW over one year (in jobs/MW) as follows:

$$OM = \frac{OM_I}{P_I} \tag{15}$$

where

OM_I is the number of jobs required for the operation and maintenance of a reference installation in a year (jobs-year); and

P_I is the power capacity of the reference facility (MW).

The previous terms also apply to Equation (16) as follows:

$$Ie = \left[\frac{CIM}{t} + OM \right] \times \frac{1000}{8760 * Fp} \tag{16}$$

where,

Ie is the job indicator for renewable technology (total jobs-year/GWh);

t is the useful life of renewable technology (years); and

Fp is the plant factor of renewable technology.

2.2.8. Normalization of the Indicators

Normalization is used to standardize the effects of different units derived from the indicators. The linear scaling method for normalization has been used in various studies [29,49,54] to transform units to an interval between 0 and 1 [58]. The greatest sustainability performance is achieved when the indicator has a value of 1.

Using Equation (17), scaling is performed as follows:

$$y = \frac{x - x_{min}}{x_{max} - x_{min}} \tag{17}$$

where

y is the standardization index;

x is the current value of the indicator;

x_{min} is the minimum value of the proposed scale; and

x_{max} is the maximum value of the proposed scale.

The proposed scales are determined based on criteria that can be arbitrary; moreover, they are related to the indicators' range [29]. For this study, the scales described in Table 4 are applied.

Table 4. The indicator standardization parameters.

| Indicator	x_{max}	x_{min}	Units
Autarchy	0	1	
Energy price	10	400	USD/BOE
Average energy price	40	70	USD/BOE
Use of RE in the energy supply	0.1	0.5	
Use of RE in the electric power supply	1	0	
Purity of energy	1	0	t CO_2/BOE
Employment	1000	300	Year-jobs

3. Results

3.1. PV Potential

Many sizing methodologies are based on municipal information, which is dependent on existing data and their accuracy [59]. Several studies use the ratio of the roof area to the ground floor area as a baseline indicator [60,61] in circumstances where sloping roofs and eaves prevail, which is common in Cuenca. The density in Cuenca is much lower than that in some other locations, such as in the Dutch case [62], where the occupancy and shadows are consistent; or the Korean case, where the facades must be included to achieve significant production [63]. Based on city cadasters, a construction occupancy of approximately 13.79 km² [64] is defined as the ground floor area, which corresponds to 166,630 of the cadastral units. Therefore, after applying the roof-to-ground-floor ratio of 1.2, the estimated roof area is 16.56 km², which corresponds to 22.64% of the urban area.

3.1.1. Reduction Factors Caused by Architectural Availability

The construction constraint (C_{con}) is considered to be 0.8 for flat roofs and 0.9 for sloped roofs. To estimate the solar potential, an average of 0.85 is used in this study [45]. To increase the accuracy, future studies should obtain more precise indicators of the proportions of flat and sloped roofs; however, such precision would require extensive statistical work and data collection. Of the total area in Cuenca, 2.14 km² is a historic area [65], and because of the architectural connotation, such areas are not considered suitable for PV application. Historic areas correspond to 2.93% of the urban area, with C_{prot} = 0.97.

Considering the restrictions due to the shadow effect, Romero and others [45] assume a C*so* factor of 0.80 for sloped roofs and 0.7 for flat roofs. These data are conservative because the incidence of shadows may be reduced due to the sun path in this region. Therefore, an average of 0.75 is assumed, considering that both types of roofs are installed. In addition, the urban density is low [66], and solar exposure at a high altitude implies that the shadow incidence is lower in equatorial latitudes [67]. Finally, because of the lack of other restrictions on the placement of PVs, C_{FV} is considered to be one.

To determine the restrictions caused by the orientation C*or* and inclination C*in*, the system advisor model (SAM) developed by the National Renewable Energy Laboratory is applied [68]. Changes in the irradiation at different inclinations and orientation angles are identified. The average annual irradiation is obtained for each azimuth (0–315°) from the average daily and monthly values (Figure 5). In Figure 6, the average annual irradiation values for different inclination angles (0–30°) are shown.
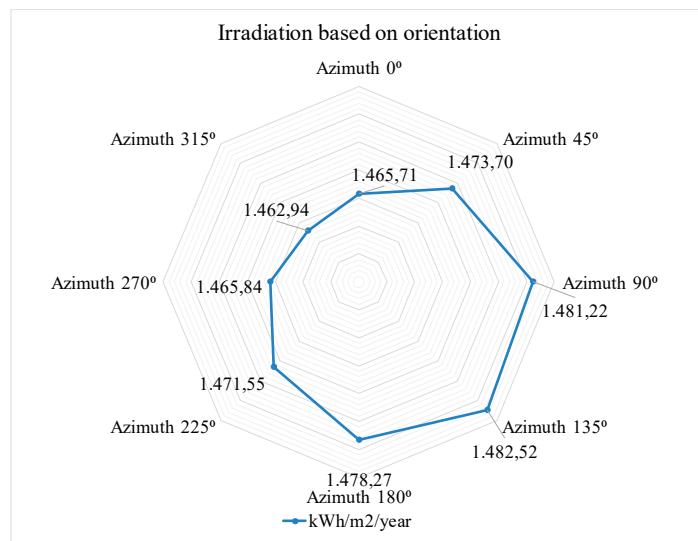
Figure 5. The average irradiation for different orientations.
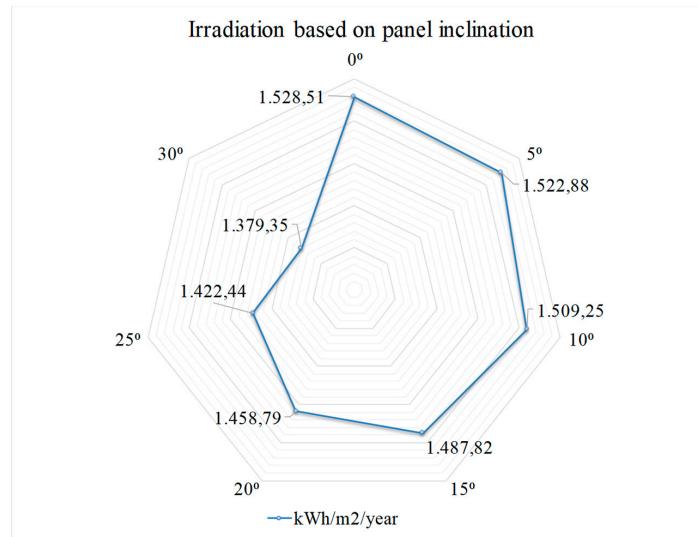
Figure 6. The average annual irradiation for different photovoltaics (PV) inclinations.

The average annual irradiation on a horizontal surface in the city is 1528.51 kWh/m^2. Comparing the minimum and maximum irradiation values when the orientation varies, a 3 to 4% variation is observed under the different orientations of the PV panels. Adopting the most critical case, *Cor* = 0.96 is used. When analyzing the inclination, a difference of up to 10% is observed between the maximum

and minimum irradiation values. Similarly, the most critical case, *Cin* = 0.90, is adopted for restrictions from the inclination.

The distance required to avoid shadows between the PVs and their maintenance paths is calculated with the methodology suggested by Byrne et al. [59]. The ground coverage ratio (GCR) is calculated using Equation (19) as follows:

$$GCR = \frac{c}{d} = \left(\cos(\beta) + \frac{b}{a} * sen(\beta) \right)^{-1} \tag{18}$$

where (Figure 7)

　　b is the space between rows;

　　a is the vertical distance;

　　β is the inclination angle of the panel;

　　c is the width of the PV panel; and
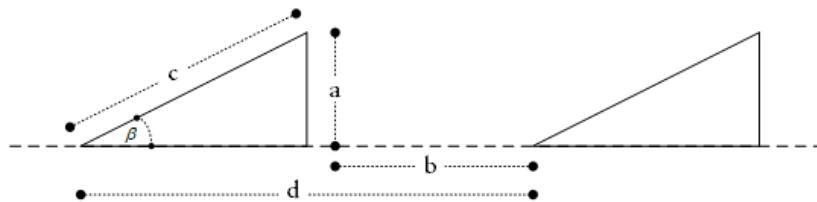
　　d is the distance between rows.

Figure 7. The ground coverage coefficient.

In practice, the ratio of b/a is expected to be 2:1 in low latitude regions and 3:1 in midlatitude regions [69]. The irradiation at the study site would be at a maximum with a nearly horizontal inclination. However, pluvial cleaning is an important factor when considering inclination, and dirt accumulations are usually maintained at under 1% in areas with constant rainfall, such as Cuenca [70,71]. In Table 5, different ground coverage coefficients for different angles are provided to determine the service area for access and maintenance (C_{SM}). At smaller angles, a specific spacing area must be provided, whereas, for greater angles, the spacing required to avoid losses can be used as the service area. Byrne et al. [59] proposed a spacing of 20% when the inclination angle is minimal and a linear reduction to 0% for a 30° inclination.

Table 5. The ground coverage coefficient and service area.

Beta	b/a = 2:1			b/a = 3:1		
	GCR (%)	SA (%)	C_{SM} (%)	GCR (%)	SA (%)	C_{SM} (%)
0	100%	20%	80%	100%	20%	80%
5	85%	17%	69%	80%	17%	63%
10	75%	13%	62%	66%	13%	53%
15	67%	10%	57%	57%	10%	47%
20	62%	7%	55%	51%	7%	44%
25	57%	3%	54%	46%	3%	43%
30	54%	0%	54%	42%	0%	42%

According to Table 5, for regions with a low latitude ratio of 2:1 and a 10° inclination, the restrictions for the separation of panels (GCR) and the area for accessibility and maintenance (C_{SM}) are 0.62 for flat roofs [59,69] and 1 for sloped roofs. For this study, the average value of 0.81 is used.

The area intended for solar collectors is calculated using Equation (19) as follows [72,73]:

$$E_{th} = A_{st} \times I \times \eta_{th} \tag{19}$$

where

E_{th} is the energy required for water heating in kWh/year;

A_{st} is the surface area in m²;

I is the average irradiation in kWh/m²/year considering different inclinations (0–30°) and orientations (0–315° in relation to the azimuth) (1472.72 kWh/m²/year); and

η_{th} is the solar collector efficiency.

The hot water consumption for an average household (four inhabitants in Cuenca) is 2065.70 kWh/year. Based on the average local irradiation and 65% efficiency, the required surface is 2.16 m²/home. Based on an additional area of 20% for maintenance, the total required area for 107,598 households will be 0.27 km² (0.39% of Cuenca's area). Therefore, the required coefficient for the solar collector systems is CST = 0.99.

Table 6 summarizes all the described reduction factors used for the calculation of the available area.

Table 6. The utilization factors used for the calculation of available roof surface.

Reduction Factor	Value	Source
C_{con}	0.85	[45]
C_{prot}	(1−2.14/73) = 0.97	[65]
C_{so}	0.75	[45]
C_{or}	0.96	Evaluation with SAM software for different orientations.
C_{in}	0.90	Evaluation with SAM software for different inclinations.
C_{SM}	0.81	[59,69]
C_{FV}	1	
C_{ST}	(1−0.27/16.56) = 0.98	Calculated based on ACS demand
F_r	0.426	Equation (2)

3.1.2. Solar Potential Reduction Indexes

Khan and Arsalan and Pelland and Poissant [74,75] proposed an efficiency of 12%, whereas Orehounig and colleagues [76] used a value of 23%. For this study, η_{ef} = 0.18 is considered. Although losses from weather are important, they are not locally applicable; however, the SAM simulation and irradiation statistics consider cloudiness from climate records. Therefore, η_{te} = 0.90 is used, which is taken from the literature [45,46]. Losses from the incidence of solar radiation on the panels are 0.95 for nonoriented surfaces and 1 for oriented surfaces. The average value η_{or} = 0.97 is applied for all orientations. Considering the losses from reflection, dust, dirt or connections, 0.84 is assumed, as proposed by Bergamasco and Asinari [46]. Table 7 presents a summary of the proposed factors.

Table 7. The factors that reduce the solar potential.

Reduction Factor	Value	Source
η_{ef}	0.18	[75,76]
η_{te}	0.90	[45,46]
η_{or}	0.97	[45]
η_{in}	0.84	[46]
η_r	0.13	Equation (3)

3.1.3. PV Solar Potential

Equation (1) is used to calculate the solar potential for the urban city of Cuenca. The reduction coefficient for the conditions of PV occupancy is 0.43. In Table 8, the results for the estimated roof area

and the reduction factors are summarized. A theoretical potential of 1454.90 GWh/year is expected for all the roofs registered by the municipality up to 2015.

Table 8. The photovoltaic solar potential in the city of Cuenca.

Parameter	Value	Unit
Floor area	13.79	km^2
Roof area/ground floor area	1.20	
Roof area	16.55	km^2
Fr	0.43	
ηr	0.13	
Average annual irradiation (horizontal surface)	1528.51	kWh/m^2
Solar energy potential in the urban city of Cuenca	1454.90	GWh
Demand for energy power in the city of Cuenca	423.80	GWh
Distribution losses	31.89	GWh
Electric power supply capacity by photovoltaic	319.27	%

In 2015, the electric power required to meet the demand of the urban area in Cuenca city was 455.70 GWh (262.39 kBOE). The overall potential of integrated PVs is to supply 3.19 times the electric power demand for the base year. The total power of the PV plant would be 314.27 MW, with a plant factor of 16.55% (1450 h). These values are a quick estimate to obtain a probable magnitude under conservative scenarios for applying the loss coefficients.

Table 9 includes this potential in the energy balance of the city of Cuenca. In this case, all the electricity is provided by the PVs. However, considering the demand, only 9% of all urban energy consumption will be satisfied because energy consumption is dominated by transportation fuel needs.

**Table 9.** The energy balance E$_{S1}$ (kBOE).

	EP *	NG	GA	DI	OF	GLP	Solar	Total
Production	0.00	0.00	0.00	0.00	0.00	0.00	1567.41	1567.41
Import	0.00	59.47	984.85	789.35	218.49	402.46	0.00	2454.62
Export	0.00	0.00	0.00	0.00	0.00	0.00	0.00	0.00
Total supply	0.00	59.47	984.85	789.35	218.49	402.46	1567.41	4022.03
Power plants (FV)	282.13	0.00	0.00	0.00	0.00	0.00	−1567.41	−1285.28
Distribution	−19.75	0.00	0.00	0.00	0.00	0.00	0.00	−19.75
Total transformation	262.39	0.00	0.00	0.00	0.00	0.00	−1567.41	−1305.03
Residential	102.34	0.00	0.00	0.00	0.00	270.39	0.00	372.73
Industry	61.89	59.47	0.00	127.33	216.55	98.68	0.00	563.92
Transportation	0.00	0.00	984.83	642.73	0.00	0.00	0.00	1627.56
Commercial	59.62	0.00	0.00	0.00	0.00	25.89	0.00	85.51
Street lighting	18.56	0.00	0.00	0.00	0.00	0.00	0.00	18.56
Other	19.98	0.00	0.02	19.29	1.93	7.49	0.00	48.72
Total demand	262.39	59.47	984.85	789.35	218.49	402.46	0.00	2717.00

* EP, Electric power; GN, natural gas; GA; Gasoline; DI, diesel; OF, oil fuel, LPG, liquefied petroleum gas.

In Figure 8, the Sankey diagram corresponding to Table 9 is shown. The solar photovoltaic use is represented as a photovoltaic plant. Losses correspond to solar energy that is not used due to the efficiency of the panels. Under this approach, the urban energy model indicated in Figure 4 is modified as shown in Figure 9 [41]. In this case, there is a new paradigm, because it is assumed that energy can be produced within the limits of the city. Now, using the indicators defined in the previous section, the impact of including PV energy in the city is determined.
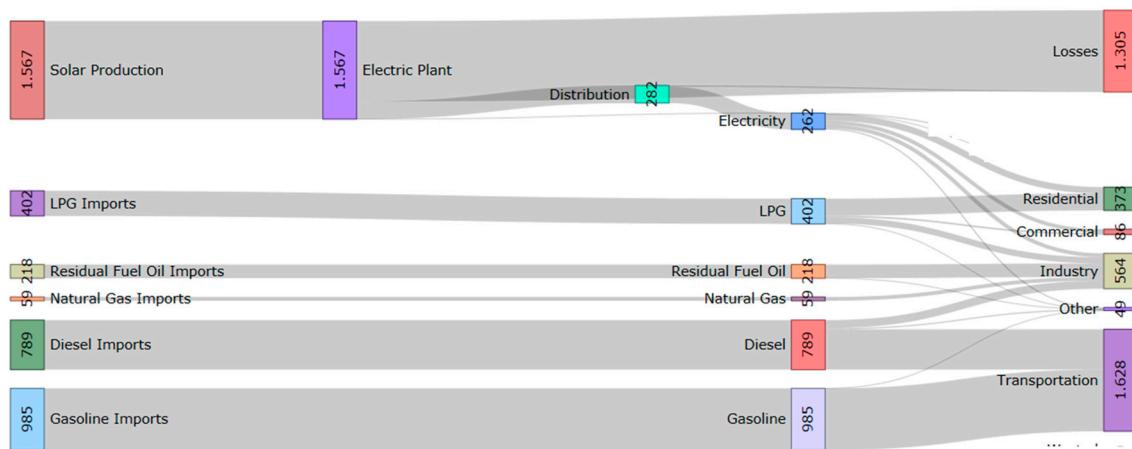
Figure 8. The Sankey diagram of the energy situation of Cuenca after taking advantage of photovoltaic solar energy.
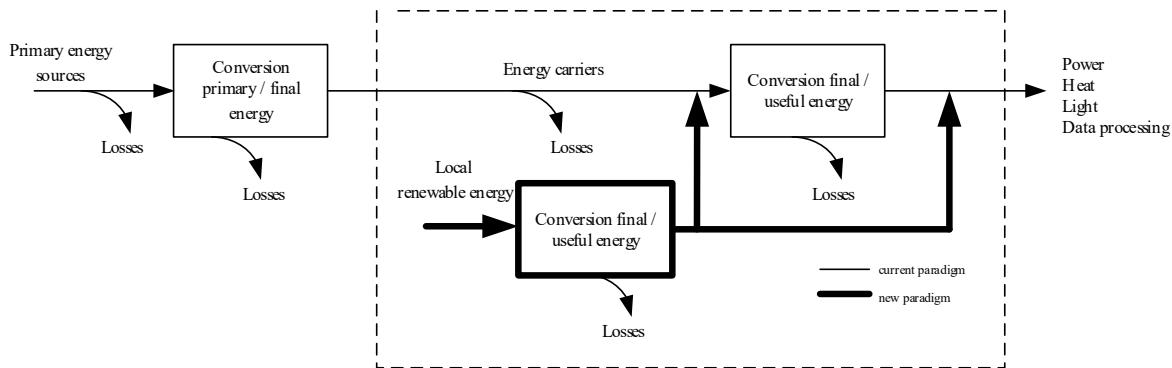
Figure 9. The current and suggested energy models (courtesy: WIT Press).

3.2. Sustainability Indicators

3.2.1. Energy Autarchy

Using energy autarchy (Equation (4)), the degree of dependence on energy imports is assessed. In Table 10, the information required for the calculation of the indicator and the standardized autarchy AEn are shown. In this case, the intensive use of PV panels (E_{S1}) enables a 100% energy self-sufficiency for the electric power requirement and a standardized autarchy of 10.28%.

Table 10. The energy autarchy in different scenarios.

Scenario	IEp + IEs (MBOE)	OE (MBOE)	AE	AEn (%)
E_{S0}	2736.75	2,736.75	1.00	0.00%
E_{S1}	2455.83	2736.75	0.90	10.28%

3.2.2. Price

The investment in PV systems is calculated with Equation (5) and shown in Table 11. In Table 12, the cost (Ce) of electricity, calculated using Equation (6), is shown. The investment cost of the PV systems is obtained using the operating cost, a 1.2% financing rate on investment [77] and a discount rate of 10%, which indicates a high risk as proposed by the IEA/NEA (2015).

Table 11. The investment in photovoltaic (PV) systems.

Base Cost (USD/kW)	S_2 (MW)	C_{T2} (M USD)	Reference	S_1 (MW)	p	C_{T1} (USD/kW)	C_{T1} Average (USD/kW)
2240.00	0.90	2.02	[50]	1.00	0.75	2181.77	1433.79
2371.00 *	0.01	0.02	[52]			685.81	

Table 12. The cost of energy produced by solar PV systems.

Scenario	Inv. (USD/kW)	O&M (USD/kW)	r (%)	Useful Life (years)	Power (MW)	Plant Factor (%)	Ce (USD/kWh)
E_{S1}	1433.79	17.2	10	25	314.27	16.55	0.12

The price of electricity and the standardized indicator (PEn) are calculated from Equations (8) and (17) (Table 13). For all energy resources, the profit (Ut) increases by 15%. For fossil fuels, the profit increases by 12% due to the value-added tax (VAT Ecuador). In the case of electricity, the VAT is 0%.

Table 13. The price of electricity from PVs.

Scenario	Ce (USD/kWh)	Ce (USD/BOE)	VAT (%)	Profit (%)	PE (USD/BOE)	PEn (%)
E_{S1}	0.12	196.72	0.00	0.15	226.23	44.56%

The price of energy resources including fossil fuels and electricity in Ecuador are identified in Table 14 (baseline scenario E_{S0}).

Table 14. The price of energy resources in Ecuador.

Energy Resource	Price	Unit	Source	PE (USD/BEP)	PEn (%)
E_{S0} Elec	0.0933	USD/kWh	[78,79]	150.71	63.92%
Es_0 domestic LPG	0.1066	USD/kg	[79,80]	13.10	99.20%
Es_0 industrial LPG	0.638	USD/kg	[80]	78.42	82.46%
Es_0 industrial NG	8.39	USD/MMBtu	[81]	46.29	90.70%
E_{S0} domestic gasoline	1.30	USD/gallon	[80]	60.24	87.12%
E_{S0} industrial gasoline	1.49	USD/gallon	[80]	69.04	84.86%
E_{S0} residential diesel	0.90	USD/gallon	[80]	36.68	93.16%
E_{S0} industrial diesel	1.32	USD/gallon	[80]	52.58	89.08%
E_{S0} fuel oil	0.80	USD/gallon	[80]	32.19	94.31%

3.2.3. Average Price of Energy to the Final Consumer

The average price of energy to the consumer is calculated via Equation (8). In Table 15, the prices (ΣPe_j*E_j), energy (E_j), average price (PME) and standardized average price (PMEn) are shown. The placement of PVs (E_{S1}) affects the indicator because it is half the value of E_{S0}.

Table 15. The average price of energy.

Scenario	ΣPe_j*E_j (M USD)	ΣE_j (k BOE)	PME (USD/BOE)	PMEn (%)
E_{S0}	150.846.74	2717.00	55.52	48.27%
E_{S1}	170.662.80	2717.00	62.81	23.96%

3.2.4. The Use of REs in the Energy Supply

Equation (9) is used to calculate the indicator that measures the impact of including energy resources from PV systems (E_{S1}) in the urban energy matrix. Table 16 shows the use of REs and the energy supply (OE, in Spanish).

Table 16. The use of renewable energies (Res) in the energy supply.

Scenario	RE (kBOE)	OE * (kBOE)	UR	URn (%)
E_{S0}	0.00	2736.75	0.00	0.00%
E_{S1}	282.13	2736.75	0.10	10.31%

* Energy supply is equal to demand plus losses.

3.2.5. The Use of REs in the Electric Power Supply

For the conventional production of electricity, Equation (10) is applied. Table 17 shows the production of electricity with REs (ERe), the electric power supply (OEe), the contribution of the RE (URe), and the standardized indicator (URen). When analyzing this indicator and the intensive use of PV, electricity requirements are considered.

Table 17. The use of REs in the electric power supply.

Scenario	ERe (kBOE)	OEe (kBOE)	URe	URen (%)
Es_0	0.00	282.13	0.00	0.00%
Es_1	282.13	282.13	1.00	100.00%

3.2.6. Energy Purity

Table 18 shows the energy purity indicator (PR*e*) and the standardized indicator (PR*en*), which are calculated with Equations (11) and (17), respectively. The table shows the carbon dioxide emissions (C*EC*) derived from Equation (12) and the energy demand (DE). This indicator does not show improvement relative to the baseline case, and the sectors related to emissions are not affected by the inclusion of PVs at an urban level.

Table 18. Energy purity.

Scenario	CEC (kT CO_2)	DE (kBOE)	PRe (t CO_2/BOE)	PRen (%)
Es_0	987.29	2717.00	0.363	34.16%
Es_1	987.29	2717.00	0.363	34.16%

To evaluate the emissions produced by electric power generation, the emission factor of the Ecuadorian electrical sector (0.6945 t CO_2/MWh = 1.12 t CO_2/BOE) is considered [82]. In the baseline case, E_{S0}, 0.317 kT CO_2 is produced from the electrical sector, which is 0.03% of the total emissions in Cuenca. This finding indicates that the emissions from electric power generation are not significant when evaluating the energy purity indicator, and they are only relevant in the case of replacing fuel consumption within urban limits.

3.2.7. Employment

Regarding jobs from the energy sector, the job factors I*e* are shown in Table 19. Jobs from conventional sources are shown in Table 20. In Table 21, estimates of the number of jobs (Em) are shown, and the standardized indicator (Emn) is calculated with Equations (16) and (17) for each scenario. Massive PVs would significantly increase the indicator (E_{S1}).

Table 19. The employment indicator (electric power production).

CIM (People-Year /MW)	*OM* (Jobs /MW)	Reference	*Fp*	*Ie* Jobs/GWh	*Ie* Average Jobs/GWh
37.00	1.00	[57]		1.71	
32.34	0.37	[57]		1.15	
7.14	0.12	[57]	0.17	0.28	1.29
34.6	2.70	[83]		2.82	
19.7	0.70	[84,85]		1.03	
25.9	0.10	[86]		0.78	

Table 20. The use of traditional energy resources.

System	*Ie* (Total Jobs-Year/GWh)	Source	*Ie* (Total Jobs-Year/GWh)
Hydroelectric power *	0.05	[85]	0.05
Fossil fuel electric power *	0.11	[57]	0.11
Fossil fuels **	0.05	[85]	0.07
	0.09	[57]	

* The average number of jobs for electric power coming from outside the city is considered. ** For fossil fuels, Rutovitz et al. [85] suggest using the same factors as for NG.

Table 21. Employment.

Scenario	Em (Jobs-Year)	Emn (%)
Es_0	315.00	2.14%
Es_1	866.40	80.91%

3.2.8. Comparison of Energy Indicators for Cuenca

Standardized indicators are grouped to provide an overall evaluation for each scenario. In Figure 10, a summary of the previously presented results is shown. According to the graph, autarchy (AEn) is increased by including PVs, and the same result is obtained with the use of REs (URn) overall. The indicator measuring the use of electricity (URen) reaches 100%. In the baseline scenario (E_{S0}), the indicator related to the average energy price (PMEn) slightly exceeds that of scenario E_{S1}, in which the average price increases. Emissions remain uniform (PRen) since the use of fossil fuels within the city is unchanged. In the case of jobs (Emn), PV technology exhibits a significant impact, although PV production only replaces electricity.
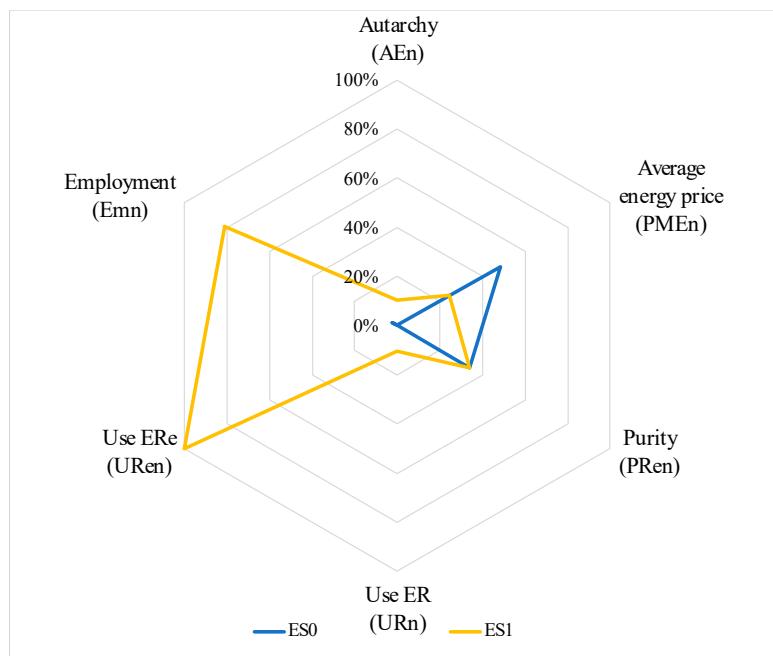
Figure 10. The comparison of sustainability energy indicators.

4. Discussion

Compared with centralized REs (solar farms or wind farms occupying 45 km^2/GWh and 72 km^2/GWh, respectively) [87], renewable energy in cities reduces human intervention and pollution outside the city limits. Given the irregularity of some renewable resources, mismatched consumption-production strategies should be implemented and the storage capacity must be improved [88]. Large-scale RE within cities is a recent type of application. Consequently, it is necessary to identify its impacts prior to proposing policies for RE use. The goal of this research is to analyze the impact of a massive implementation of PVs in an urban area. The results show that even when the potential for RE can meet the demand for electricity, its influence on the urban energy matrix is marginal. The methodology used to estimate the potential provides a rapid evaluation of the approximate size of the urban PV potential using municipal data for cities with limited resources, such as those in developing countries. This methodology is better suited for an equatorial location, where the totality of the sloped roofs can be used considering that a sloped roof oriented to any direction irradiates evenly.

The calculated potential indicates that the availability of solar energy for the purpose of electricity production is close to three times higher than the demand for electricity. The studies mentioned in Table 1 presented positive results because of the seasonality, solar radiation and low building consumption for environmental conditioning. These results are comparable to the results of a more detailed study that used 3D roofing models and obtained the precise production demands at daily and monthly scales. However, the previous study corresponds to the commercial sector of the city, and it obtained a PV potential close to 150% of the demand [42]. In an industrial area with high consumption, the value decreases to 22% [89].

In Cuenca, solar resources stand out because of the absence of seasonal variations and the comparatively stable energy demand throughout the year, which reduces the required storage. Another feature is the minimal reduction in performance from the inclination and orientation of the PVs, and furthermore, the dispersed growth of the city increases the potential compared to more compact cities. Based on the total estimated area, approximately 42.25 m^2 of roof area is available per inhabitant, whereas in Spain, this same proportion is only 13 m^2 [27], and this difference is primarily because single-family homes are more popular in Cuenca. The estimated potential shows that the entire

electricity demand can be met with PVs. However, a smart grid and some network adaptations are required to control the intermittencies of production and consumption [79]. Moreover, solar power represents a good complement to hydropower, which is the main source of the Ecuadorian electricity supply.

In most cities, the use and destination of the energy for consumption are unknown [90]. Although the energy requirements of cities are not fully known, the impact cannot be established by applying policies that propose a change in the urban energy model [3].

As has been done at the country level, it is necessary to determine the real impact of adding renewables into the urban energy mix. Most studies review the incidence of PV electricity production, but this research shows that a holistic analysis is essential to establish its real impact. The novelty of this study is that it proposes and measures the impact of electricity self-production using sustainability indicators.

Several international proposals promote renewables adoption in cities [2,5]. Despite this interest, methods for measuring the change in the urban energy model have not been established [3,91]. There are several urban indicators, including those that measure the management and use of energy, but few are directed to comprehensively evaluate the use of renewables within cities. Therefore, sustainable energy indicators that are usually used at the country or regional level and that are compatible with the proposal of this research were identified.

It is unlikely that a city will achieve total energy self-sufficiency by using only endogenous resources, at least in the short term. Although the importation of energy based on fossil resources does not diminish substantially, the average prices of energy are not substantially altered and may even increase markedly. This is evidenced by a reduction in the PMEn indicator.

The use of renewable energy will still require the import of energy, but it could replace 100% of the electricity requirement. This ability, however, does not alter the energy purity because the urban matrix is highly influenced by transport and fossil fuels. Despite this, the indicator that measures employment with the intensive use of PV solar energy is favoured. The urban energy matrix traditionally maximizes energy use based on fossil fuels. In the case of Cuenca, with the evaluated technology, this energy model has not been modified. Therefore, aside from renewable energies, there are other inescapable strategies that must be embraced (energy efficiency programs, passive strategies, or changes to consumer equipment, especially to electric transport). However, any proposal that seeks to change the way the city is projected must involve authorities, planners or citizens.

In Ecuador, the real price for the production and distribution of electricity is Pe = USD 0.09, and it is reduced to USD 0.04 after public subsidy. This price does not consider the cost of hydroelectric dams, whose construction has been subsidized by public investment. Because the costs of hydroelectric energy are highly subsidized and the production of photovoltaic energy must currently consider taxes on imported equipment, the latter becomes noncompetitive [79]. Compared to the estimated price, the PV cost is USD 0.12 per kWh, meaning that this source would not be feasible. For this reason, investments and energy costs are decisive factors [92]. However, considering future electricity growth, PV becomes more attractive because of the rapid price reduction. The use of PV systems also avoids the impact on natural resources; therefore, the subsidies previously applied to hydroelectric energy could be transferred to PVs or other energy alternatives.

5. Conclusions

The estimated potential, determined using information from the study area, requires a deeper analysis that includes technical, environmental, and economic aspects, which could be limiting factors to the extensive implementation of each technology. However, the results are an appropriate starting point. Reduction factors in the area of application represent the primary drawbacks that could affect the calculation of the PV potential using the proposed methodology. However, a deeper analysis is beyond the scope of this research because of the diverse roof characteristics, directionality, inclination, shadows, obstacles and city size, which must all be considered in areas where solar capture is possible.

Nevertheless, the information used to obtain the indicators is useful for measuring the impact of PVs on the energy requirements of the city.

In Cuenca, PV technology would be more prevalent if there was a reduction in incoming energy flows, and the autarchy indicator could reach AEn = 10.28%. This result would impact the average price of electricity compared with the baseline scenario (PMEn = 48.27%) since the price increased with PV solar energy when the indicator value was reduced to 23.96%. As previously mentioned, substitution does not affect urban emission limits, since the use of fossil fuels is minimally altered. Furthermore, PV technology would increase EMn, which measures the employment rate (over 78% with respect to the baseline case). The indicator that measures the incidence of renewables (URn) in the energy matrix indicates that even with the massive provision of electricity via PVs (URen = 100%), the city would continue to depend on external resources for approximately 90% of its needs. Achieving the maximum self-sufficiency requires a change in transport systems from fuel to electrical transport systems and the maximization of electrical equipment in buildings.

The indicators used here have been applied to countries rather than cities since cities have not traditionally been considered a source of energy. However, due to current technology, the urban energy model can be changed based on the use of resources available to a city. The proposed indicators are useful at an urban scale because they can be used to assess the real impact of policies designed to decarbonize cities.

The main contribution of this study is a method for evaluating PV solar potential that does not require significant human or computational resources. However, this method may not be as useful or as accurate for other regions where the orientation and inclination of panels are more critical. Based on urban sustainability indicators, this study also evaluates the impact of electric power provision on the entire energy system. The results show that substituting electricity with renewable sources will not solve the urban energy problem. A complete and detailed evaluation is required to encourage the use of other REs in applications such as transportation and heating, and to promote the use of equipment that consumes electricity or nonfossil fuels.

References

1. Bai, X.; Dawson, R.J.; Ürge-Vorsatz, D.; Delgado, G.C.; Salisu Barau, A.; Dhakal, S.; Dodman, D.; Leonardsen, L.; Masson-Delmotte, V.; Roberts, D.C.; et al. Six research priorities for cities and climate change. *Nature* **2018**, *555*, 23–25. [CrossRef] [PubMed]
2. IEA. *Cities, Towns & Renewable Energy Cities, Towns*; IEA/OECD: Paris, France, 2009.
3. IRENA. *Renewable Energy in Cities*; IRENA: Abu Dhabi, UAE, 2016.
4. IRENA. *REthinking Energy*; IRENA: Abu Dhabi, UAE, 2017; Volume 55.
5. Barragán-Escandón, A.; Terrados-Cepeda, J.; Zalamea-León, E. The Role of Renewable Energy in the Promotion of Circular Urban Metabolism. *Sustainability* **2017**, *9*, 2341. [CrossRef]
6. IEA. *Cities, Towns & Renewable Energy: Yes in My Front Yard*; IEA/OECD: Paris, France, 2009.
7. Mainzer, K.; Killinger, S.; McKenna, R.; Fichtner, W. Assessment of rooftop photovoltaic potentials at the urban level using publicly available geodata and image recognition techniques. *Sol. Energy* **2017**, *155*, 561–573. [CrossRef]

8. Caldarelli, C.E.; Gilio, L. Expansion of the sugarcane industry and its effects on land use in São Paulo: Analysis from 2000 through 2015. *Land Use Policy* **2018**, *76*, 264–274. [CrossRef]

9. Poggi, F.; Firmino, A.; Amado, M. Planning renewable energy in rural areas: Impacts on occupation and land use. *Energy* **2018**, *155*, 630–640. [CrossRef]

10. Dilimulati, A.; Stathopoulos, T.; Paraschivoiu, M. Wind turbine designs for urban applications: A case study of shrouded diffuser casing for turbines. *J. Wind Eng. Ind. Aerodyn.* **2018**, *175*, 179–192. [CrossRef]

11. Barragán, E.A.; Terrados, J.; Zalamea, E.; Arias, P. Electricity production using renewable resources in urban centres. *Proc. Inst. Civ. Eng.* **2017**, in press.

12. Compagnon, R. Solar and daylight availability in the urban fabric. *Energy Build.* **2004**, *36*, 321–328. [CrossRef]

13. Kaan, H.; Reijenga, T. Photovoltaics in an architectural context. *Prog. Photovolt. Res. Appl.* **2004**, *12*, 395–408. [CrossRef]

14. Castro, M.; Delgado, A.; Argul, F.J.; Colmenar, A.; Yeves, F.; Peire, J. Grid-connected PV buildings: Analysis of future scenarios with an example of Southern Spain. *Sol. Energy* **2005**, *79*, 86–95. [CrossRef]

15. Hafeez, S.; Atif, S. 3D Rooftop Photovoltaic Potential Calculation Using GIS Techniques: A Case Study of F-11 Sector Islamabad. In Proceedings of the 2014 12th International Conference on Frontiers of Information Technology, Islamabad, Pakistan, 17–19 December 2014; pp. 187–192.

16. Liang, J.; Gong, J.; Zhou, J.; Ibrahim, A.N.; Li, M. An open-source 3D solar radiation model integrated with a 3D Geographic Information System. *Environ. Model. Softw.* **2015**, *64*, 94–101. [CrossRef]

17. Kanters, J.; Wall, M.; Dubois, M.-C. Typical Values for Active Solar Energy in Urban Planning. *Energy Procedia* **2014**, *48*, 1607–1616. [CrossRef]

18. Eicker, U.; Klein, M. Large-scale renewable energy integration within energy-efficient urban areas: Results from three German case studies. *Int. J. Low-Carbon Technol.* **2014**, *9*, 202–213. [CrossRef]

19. Eicker, U.; Monien, D.; Duminil, É.; Nouvel, R. Energy performance assessment in urban planning competitions. *Appl. Energy* **2015**, *155*, 323–333. [CrossRef]

20. Agudelo-Vera, C.M.; Leduc, W.R.W.A.; Mels, A.R.; Rijnaarts, H.H.M. Harvesting urban resources towards more resilient cities. *Resour. Conserv. Recycl.* **2012**, *64*, 3–12. [CrossRef]

21. Leduc, W.R.W.A.; Van Kann, F.M.G. Spatial planning based on urban energy harvesting toward productive urban regions. *J. Clean. Prod.* **2013**, *39*, 180–190. [CrossRef]

22. Fath, K.; Stengel, J.; Sprenger, W.; Wilson, H.R.; Schultmann, F.; Kuhn, T.E. A method for predicting the economic potential of (building-integrated) photovoltaics in urban areas based on hourly Radiance simulations. *Sol. Energy* **2015**, *116*, 357–370. [CrossRef]

23. Mavromatidis, G.; Orehounig, K.; Carmeliet, J. Evaluation of photovoltaic integration potential in a village. *Sol. Energy* **2015**, *121*, 152–168. [CrossRef]

24. Gautam, B.R.; Li, F.; Ru, G. Assessment of urban roof top solar photovoltaic potential to solve power shortage problem in Nepal. *Energy Build.* **2015**, *86*, 735–744. [CrossRef]

25. Eicker, U.; Nouvel, R.; Duminil, E.; Coors, V. Assessing Passive and Active Solar Energy Resources in Cities Using 3D City Models. *Energy Procedia* **2014**, *57*, 896–905. [CrossRef]

26. Jamal, T.; Ongsakul, W.; Singh, J.G.; Salehin, S.; Ferdous, S.M. Potential rooftop distribution mapping using Geographic Information Systems (GIS) for Solar PV Installation: A case study for Dhaka, Bangladesh. In Proceedings of the 2014 3rd International Conference on the Developments in Renewable Energy Technology (ICDRET), Dhaka, Bangladesh, 29–31 May 2014; pp. 1–6.

27. Koo, C.; Hong, T.; Park, H.S.; Yun, G. Framework for the analysis of the potential of the rooftop photovoltaic system to achieve the net-zero energy solar buildings. *Prog. Photovolt. Res. Appl.* **2014**, *22*, 462–478. [CrossRef]

28. OLADE. *Manual de Planificación Energética*; OLADE: Quito, Ecuador, 2014.

29. MEER. *Elaboración de la Prospectiva Energética del del Ecuador 2012–2040*; MEER: Quito, Ecuador, 2015.

30. MICSE. *Balance Energético Nacional 2016, año Base 2015*; MICSE: Quito, Ecuador, 2015.

31. OECD/IEA. *Energy Efficiency Indicators: Essentials for Policy Making*; OECD/IEA: Paris, France, 2014.

32. CEPAL/OLADE/GTZ. *Energía y Desarrollo Sustentable en América Latina y el Caribe: Guía Para la Formulación de Políticas Energéticas*; Naciones Unidas: Santiado de Chile, Chile, 2003.

33. Garcia, F.; Hernández, G.; Luna, N. *Manual de estadísticas energéticas*; Organización Latinoamericana de Energía: Quito, Ecuador, 2011; Volume 53.

34. GAD Cuenca. *Plan de Desarrollo y Ordenamiento Territorial del Cantón Cuenca*; GAD Cuenca: Cuenca, Ecuador, 2015.

35. Clasificador Geográfico Estadístico. Available online: http://www.ecuadorencifras.gob.ec/clasificador-geografico-estadistico-dpa/ (accessed on 25 February 2019).

36. Jaramillo, C. *Estudio de Metabolismo Urbano en la Ciudad de Cuenca*; Universidad Politécnica Salesiana: Cuenca, Ecuador, 2017.

37. NREL System Advisor Model (SAM). Available online: https://sam.nrel.gov (accessed on 12 June 2018).

38. Centrosur. *Base de Datos*; Centrosur: Cuenca, Ecuador, 2017.

39. INER. *Escenarios de Prospectiva Energética para Ecuador a 2050*; INER: Quito, Ecuador, 2016.

40. Ministerio Coordinador de Sectores Estratégicos. *Matriz Energética*; Ministerio Coordinador de Sectores Estratégicos: Quito, Ecuador, 2013.

41. Barragán, E.; Terrados, J.; Barragán, A.; Terrados, J.; Barragán, E.; Terrados, J. Sustainable cities: An analysis of the contribution made by renewable energy under the umbrella of urban metabolism. *Int. J. Sustain. Dev. Plan.* **2017**, *12*, 416–424. [CrossRef]

42. Zalamea-León, E.; Mena-Campos, J.; Barragán-Escandón, A.; Parra-González, D.; Méndez-Santos, P. Urban Photovoltaic Potential of Inclined Roofing for Buildings in Heritage Centers in Equatorial Areas. *J. Green Build.* **2018**, *13*, 45–69. [CrossRef]

43. Izquierdo-torres, I.F.; Pacheco-portilla, M.G.; Gonzalez-Morales, L.G.; Zalamea-Leon, E.F. Simulación fotovoltaica considerando parámetros de integración en edificaciones Photovoltaic simulation considering building integration parameters. *INGENIUS Rev. Cienc. y Tecnol.* **2019**, *21*, 9–19.

44. IDEE Balances Energéticos. *Seminario-Taller Política Energética para el Desarrollo Sustentable y el uso del Modelo LEAP*; Fundación Bariloche: Bariloche, Argentina, 2016; p. 106.

45. Romero Rodríguez, L.; Duminil, E.; Sánchez Ramos, J.; Eicker, U. Assessment of the photovoltaic potential at urban level based on 3D city models: A case study and new methodological approach. *Sol. Energy* **2017**, *146*, 264–275. [CrossRef]

46. Bergamasco, L.; Asinari, P. Scalable methodology for the photovoltaic solar energy potential assessment based on available roof surface area: Application to Piedmont Region (Italy). *Sol. Energy* **2011**, *85*, 1041–1055. [CrossRef]

47. D'Orazio, M.; Di Perna, C.; Di Giuseppe, E. Performance assessment of different roof integrated photovoltaic modules under Mediterranean Climate. *Energy Procedia* **2013**, *42*, 183–192. [CrossRef]

48. Luque, A.; Hegedus, S. *Handbook of Photovoltaic Science and Engineering Handbook of Photovoltaic Science and Engineering*; John Wiley & Sons: West Sussex, UK, 2011.

49. ESMAP. *Resultados de la Conferencia Regional Sobre Energía y Reducción de la Pobreza de la Alianza Global de Energía Comunal para América Latina y el Caribe*; ESMAP: Santa Cruz de la Sierra, Bolivia, 2003.

50. IEA/NEA. *Projected Costs of Generating Electricity*; IEA/NEA: Paris, France, 2015.

51. Joubert, E.C.; Hess, S.; Niekerk, J.L. Van Large-scale solar water heating in South Africa: Status, barriers and recommendations. *Renew. Energy* **2016**, *97*, 809–822. [CrossRef]

52. Energy Styrelsen. *Technology Data for Energy Plants. Generation of Electricity and District Heating, Energy Storage and Energy Carrier Generation and Conversion*; Energy Styrelsen: Copenhagen, Denmark, 2012.

53. IEA. *Production of Alternative Transportation Fuels: Influence of Crude Oil Price and Technology Maturity*; IEA: Paris, France, 2013.

54. Guayanlema, V.; Fernández, L.; Arias, K. Análisis de indicadores de desempeño energético del Ecuador. *Enerlac* **2017**, *1*, 121–131.

55. Zhang, L.; Feng, Y.; Chen, B. Alternative scenarios for the development of a low-carbon city: A case study of Beijing, China. *Energies* **2011**, *4*, 2295–2310. [CrossRef]

56. Heaps, C.G. *Long-Range Energy Alternatives Planning (LEAP) System 2016*; Stockholm Environment Institute: Somerville, MA, USA, 2017.

57. Wei, M.; Patadia, S.; Kammen, D.M. Putting renewables and energy efficiency to work: How many jobs can the clean energy industry generate in the US? *Energy Policy* **2010**, *38*, 919–931. [CrossRef]

58. Schuschny, A.; Soto, H. *Guía Metodológica Diseño de Indicadores Compuestos de Desarrollo Sostenible*; Naciones Unidas: Santiado de Chile, Chile, 2009.

59. Byrne, J.; Taminiau, J.; Kurdgelashvili, L.; Kim, K.N. A review of the solar city concept and methods to assess rooftop solar electric potential, with an illustrative application to the city of Seoul. *Renew. Sustain. Energy Rev.* **2015**, *41*, 830–844. [CrossRef]

60. IEA. Potential for building integrated photovoltaics. *IEA-PVPS Task* **2002**, *7*, 2–4.

61. Peng, J.; Lu, L. Investigation on the development potential of rooftop PV system in Hong Kong and its environmental benefits. *Renew. Sustain. Energy Rev.* **2013**, *27*, 149–162. [CrossRef]

62. Moraitis, P.; Bala Bhavya, K.; Nortier, N.; Van Sark, W. Urban Environment and Solar PV Performance. *Energies* **2018**, *11*, 1333. [CrossRef]

63. Oh, J.; Koo, C.; Hong, T.; Jeong, K.; Lee, M. An economic impact analysis of residential progressive electricity tariffs in implementing the building-integrated photovoltaic blind using an advanced finite element model. *Appl. Energy* **2017**, *202*, 259–274. [CrossRef]

64. GAD. *Cuenca Información catastral del Cantón Cuenca (Urbano)*; GAD: Cuenca, Ecuador, 2017.

65. El Telégrafo INPC Presentará Demanda por Demolición de Casa Patrimonial. 2013. Available online: https://www.eltelegrafo.com.ec/noticias/regional/1/inpc-presentara-demanda-por-demolicion-decasa-patrimonial (accessed on 25 February 2019).

66. Hermida, M.A.; Hermida, C.; Cabrera, N.; Calle, C. La densidad urbana como variable de análisis de la ciudad. *EURE* **2015**, *41*, 25–44.

67. Fitriaty, P.; Shen, Z. Predicting energy generation from residential building attached Photovoltaic Cells in a tropical area using 3D modeling analysis. *J. Clean. Prod.* **2018**, *195*, 1422–1436. [CrossRef]

68. NREL. *System Advisor Model*; NREL: Golden, CO, USA, 2016.

69. Whitaker, C.M.; Townsend, T.U.; Razon, A.; Hudson, R.M.; Vallvé, X. PV systems. In *Photovoltaic Science Handbook of Photovoltaic Science*; Luque, A., Hegedus, S., Eds.; John Wiley and Sons, Ltd., Publication: West Sussex, UK, 2011; pp. 841–895.

70. Smith, M.K.; Wamser, C.C.; James, K.E.; Moody, S.; Sailor, D.J.; Rosenstiel, T.N. Effects of Natural and Manual Cleaning on Photovoltaic Output. *J. Sol. Energy Eng.* **2013**, *135*, 34505. [CrossRef]

71. Ferretti, N. *White Paper—PV Module Cleaning—Market Overview and Basics*. 2018. Available online: https://www.pi-berlin.com/images/pdf/publication/White%20Paper%20-%20PV%20Module%20Cleaning%20-%20Market%20Overview%20and%20Basics.pdf (accessed on 25 February 2019).

72. Rosas-Flores, J.A.; Rosas-Flores, D.; Fernández Zayas, J.L. Potential energy saving in urban and rural households of Mexico by use of solar water heaters, using geographical information system. *Renew. Sustain. Energy Rev.* **2016**, *53*, 243–252. [CrossRef]

73. Marique, A.-F.; Reiter, S. A simplified framework to assess the feasibility of zero-energy at the neighbourhood/community scale. *Energy Build.* **2014**, *82*, 114–122. [CrossRef]

74. Pelland, S.; Poissant, Y. An Evaluation of the Potential of Building Integrated Photovoltaics in Canada. In Proceedings of the 31st Annual Conference of the Solar Energy Society of Canada (SESCI), Montreal, QC, Canada, 20–24 August 2006.

75. Khan, J.; Arsalan, M.H. Estimation of rooftop solar photovoltaic potential using geo-spatial techniques: A perspective from planned neighborhood of Karachi—Pakistan. *Renew. Energy* **2016**, *90*, 188–203. [CrossRef]

76. Orehounig, K.; Mavromatidis, G.; Evins, R.; Dorer, V.; Carmeliet, J. Towards an energy sustainable community: An energy system analysis for a village in Switzerland. *Energy Build.* **2014**, *84*, 277–286. [CrossRef]

77. Connolly, D.; Lund, H.; Mathiesen, B.V. Smart Energy Europe: The technical and economic impact of one potential 100% renewable energy scenario for the European Union. *Renew. Sustain. Energy Rev.* **2016**, *60*, 1634–1653. [CrossRef]

78. Araujo, A. Alza de tarifas eléctricas busca rebajar el subsidio. *Diairo El Comercio* **2014**. Available online: https://www.elcomercio.com/actualidad/negocios/alza-de-tarifas-electricas-busca.html (accessed on 25 February 2019).

79. Ponce-Jara, M.A.; Castro, M.; Pelaez-Samaniego, M.R.; Espinoza-Abad, J.L.; Ruiz, E. Electricity sector in Ecuador: An overview of the 2007–2017 decade. *Energy Policy* **2018**, *113*, 513–522. [CrossRef]

80. Petroecuador, EP. *Precios de Venta a Nivel de Terminal Para las Comercializadoras Calificadas y Autorizadas a Nivel Nacional Periodo*; Petroecuador EP: Quito, Ecuador, 2016.

81. Lopez Lozano, M.F. *Explotación del Gas Natural en el Sector Fabril del Parque Industrial de Cuenca*; Universidad de Cuenca: Cuenca, Ecuador, 2014.

82. Haro, L.; Oscullo, J. Factor Anual de Emisión de CO_2 Producido por el Parque Generador del Sistema Nacional Interconectado del Ecuador, mediante la Aplicación de la Metodología de la Convención Marco Sobre el Cambio Climático UNFCCC, para el Periodo 2009–2014. *Rev. Politécnica* **2016**, *37*, 7.

83. Moreno, B.; López, A.J. The effect of renewable energy on employment. The case of Asturias (Spain). *Renew. Sustain. Energy Rev.* **2008**, *12*, 732–751. [CrossRef]

84. Rutovitz, J.; Atherton, A. *Energy Sector Jobs to 2030: A Global Analysis*. 2009. Available online: https://secured-static.greenpeace.org/international/Global/international/planet-2/binaries/2009/9/energy-sector-jobs-to-2030.pdf (accessed on 26 February 2019).

85. Rutovitz, J.; Dominish, E.; Downes, J. *Calculating Global Energy Sector Jobs 2015 Methodology Update*; Institute for Sustainable Futures, University of Technology: Sydney, Australia, 2015.

86. Pembina Institute. *Canadian Renewable Electricity Development: Employment Impacts*; Pembina Institute: Vancouver, BC, Canada, 2004.

87. Shmelev, S.E.; Van Den Bergh, J.C.J.M. Optimal diversity of renewable energy alternatives under multiple criteria: An application to the UK. *Renew. Sustain. Energy Rev.* **2016**, *60*, 679–691. [CrossRef]

88. Lund, P.D. Capacity matching of storage to PV in a global frame with different loads profiles. *J. Energy Storage* **2018**, *18*, 218–228. [CrossRef]

89. Marin-López, D.; Zalamea-León, E.F.; Barragán-Escandón, E.A. Potencial fotovoltaico en techumbres de edificios industriales de alta demanda energética, en zonas ecuatoriales. *Rev. Hábitat SustenTable* **2018**, *8*, 28–41.

90. IRENA. *Habitat III High-Level Forum on Renewable Energy in Urban Settings*; IRENA: Quito, Ecuador, 2016.

91. Energycities. *30 Propuestas de Energy Cities Para la Transición Energética de Ciudades Grandes y Pequeñas*; Energycities: Brussels, Belgium, 2014.

92. Barragán, E.; Espinoza, J.L. Políticas para la promoción de las energías renovables en el Ecuador. In *Energías Renovables en el Ecuador. Situación Actual, Tendencias y Perspectivas*; Peláez Samaniego, M.R., Espinoza Abad, J.L., Eds.; Universidad de Cuenca, Gráficas Hernández: Cuenca, Ecuador, 2015.